Structure and Magnetic Properties of Iron/Iron-Oxide Nanoparticles Prepared by Precipitation from Solid State Solution

O. Milkovič[a,b], J. Gamcová[c,*], M. Sopko[a] and I. Škorvánek[d]

[a]Institute of Materials Research, Slovak Academy of Sciences, Watsonova 47, 040 01 Košice, Slovakia

[b]Institute of Materials, Faculty of Metallurgy, Technical University of Košice, Letná 9, 040 01 Košice, Slovakia

[c]Institute of Physics, Faculty of Science, P.J. Šafárik University, Park Angelinum 9, 041 54 Košice, Slovakia

[d]Institute of Experimental Physics, Slovak Academy of Sciences, Watsonova 47, 040 01 Košice, Slovakia

The influence of precipitation temperature on structural and magnetic properties of iron/iron-oxide nanoparticles is investigated. Nanoparticles were prepared by precipitation of γ-Fe precipitates in Cu–Fe solid solution and subsequently isolated by matrix dissolution. Precipitation annealing temperatures were 773, 873, and 973 K. Nanoparticles core-shell structure and morphology were characterized by X-ray diffraction, high-resolution transmission electron microscopy, and selected area electron diffraction. These measurements showed that average diameter of nanoparticles increases with precipitation temperature from 8.5 nm to 20.5 nm. The measurements of magnetization as a function of temperature and applied field have been performed by SQUID magnetometer in temperature range from 5 K to 200 K.

1. Introduction

In last period various scientific and industrial groups are devoted in development and preparation of nanostructure metal oxides like nanoparticles (NPs) [1]. The structural and magnetic properties of Fe/Fe_3O_4 NPs has been studied in different works [2–4]. The shape of the NPs depends on the preparation methods. Several studies have demonstrated the controllable synthesis of nonspherical iron oxide NPs with cubic [5, 6], hexagonal [7], and rod [8–10] morphologies. It was shown that the size of spherical Fe_3O_4 NPs prepared by hydrolysis can be in the range from 10 to 40 nm in mean diameter. With the increase of NPs mean diameter from 12 to 40 nm their coercivity drastically increased to 7.958 kA/m and the magnetic saturation to 87.7 A m^2/kg.

In this work, spherical magnetic core-shell NPs were synthesized using the precipitation process in solid state of Cu–Fe alloy. The crystalline structure and size of NPs were characterized by X-ray diffraction (XRD), high-resolution transmission electron microscopy (HRTEM), selected area electron diffraction (SAED) techniques and the magnetic properties were investigated by SQUID magnetometer.

2. Experimental procedure

The binary Cu–Fe alloy with 1.23 wt% Fe was used as starting material for a growth of the NPs. The samples were precipitation annealed in pure argon atmosphere and quenched in cold water. Temperatures of precipitation annealing were 773 K (sample K), 873 K (sample F), and 973 K (sample A). The holding time on certain temperature was 3 h. The precipitates were subsequently extracted from the parent alloy by using a chemical solution method. Observing the morphology, shape and size distribution of NPs using TEM and determining crystal state using SAED, was done on JEOL JEM-2000FX and JEOL JEM-2000SX microscope (at an acceleration voltage of 200 keV). Sample preparation for TEM involved dispersing in pure ammonia of aqueous solution and deposition of a drop of colloidal solution onto a molybdenum grid coated with a carbon film.

The XRD measurements were carried out on P02.1 experimental station located at PETRA III storage ring in DESY, Hamburg, Germany. High-energy X-ray diffraction experiments were performed in transmission geometry. The monochromatic beam had energy 59.82 keV (λ = 0.207 Å). The diffracted patterns were recorded using an image plate detector Perkin Elmer 1621 (2048 × 2048 pixels, pixel size 200 μm × 200 μm). The NPs were placed in a quartz capillary with thickness of 1 mm. One diffraction pattern was acquired in 10 s. Diffraction patterns were integrated using the FIT2D software [11]. The sample–detector distance, detector orthogonality with respect to the incoming beam was determined by fitting of reference CeO_2 powder. The measurements of magnetization as a function of temperature and applied field have been performed by a commercial SQUID magnetometer Measuring System model MPMS-XL-5 (Quantum Design, USA) equipped with 5 T superconducting magnet in temperature range from 5 K to 200 K.

---

*corresponding author; e-mail: jana.gamcova@upjs.sk

3. Result and discussion

In Fig. 1 there is shown TEM analysis of NPs annealed at different temperatures (K = 773 K, F = 873 K, A = 973 K). In each annealed state NPs are well-separated with near-spherical shape, obvious aggregation can be observed as well. The average NPs size in the case of sample A is 20.5 nm and the size of particles is relatively homogeneous. The average size of nanoparticles in sample F and K is 12.5 and 8.5 nm, respectively. NPs size distributions are in F and K cases narrower compared to sample A.
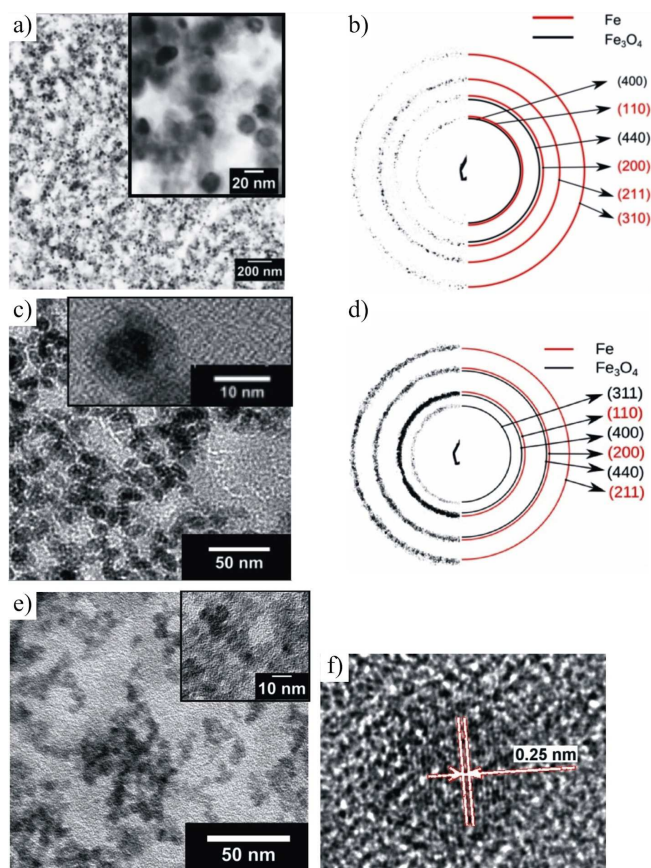
Fig. 1. TEM and SAED images of nanoparticles of sample A (a) and (b), sample F (c) and (d), TEM and HRTEM images of sample K (e) and (f).

In Fig. 1b and d there are shown SAED patterns of A and F samples. Diffraction patterns of NPs are marked by their corresponding indices of crystal planes of pure iron (α-Fe) and magnetite (Fe_3O_4) phase. Magnetite is characterized by broad diffraction rings which indicate the low crystallinity of the NPs phase.

SAED patterns and TEM images constitute the experimental evidence of the core-shell (α-Fe/Fe_3O_4) structure. The HRTEM image in Fig. 1f shows detail of K sample NPs. The measured lattice spacing is 0.25 nm which corresponds to (311) plane of the Fe_3O_4 crystalline phase. In the case of the smallest K NPs, the α-Fe in core is missing, therefore these NPs consist only from one phase

which corresponds to oxide shell Fe_3O_4, in contrast to the core-shell structure of NPs with larger diameter.

Radially integrated diffraction patterns obtained from investigated NPs are documented in Fig. 2. Profiles are refined employing the Rietveld method using two phases. Sample A and F: α-Fe (ICSD 44863; space group (S.G.) $Im3m$). Sample A, F, and K: Fe_3O_4 (ICSD 82441; S.G. $Fm3m$). Diffraction profiles show that sample K, with the smallest size distribution, is without α-Fe core. Based on differential curves can be stated that all reflections are refined and the additional phase is not presented in the diffraction patterns.
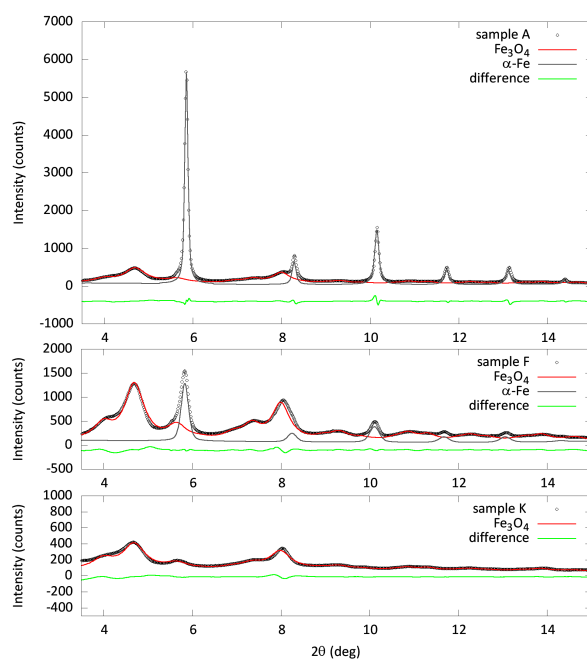
Fig. 2. XRD pattern sample A (973 K), F (873 K) and K (773 K).

Fitted structure parameters and volume ratio of the identified phases are summarized in Table I.

TABLE I

Fitted structure parameters and volume ratio of the identified phase.

	Volume [%]		Lattice parameter [Å]		Crystalline size [nm]	
	α-Fe	Fe_3O_4	α-Fe	Fe_3O_4	α-Fe	Fe_3O_4
A	40.5	59.5	2.865	8.380	15.4	2.3
F	8.5	91.5	2.883	8.401	7	2.4
K	0	100	–	8.398	0	2.3

It is very interesting to compare the lattice parameter and volume fraction of the NPs cores. Maximal lattice parameter of the α-Fe is determined for the lower volume fraction of the NPs core. We can explain this effect by lattice deformation at the core–shell interface after the oxidation of NPs during the isolation process. While noble NPs are uncovered by chemical dissolution of Cu

matrix, NPs surface is passivated by oxidation. Passivated layer is formed in core–shell interface and generates lattice strains in the core volume close to the interface. Effect of strained lattice is more evident in increase of lattice parameter value if there is higher ratio between strained volume and overall volume of the core or in case the average NPs size is larger.

Rate of passivation process is too high for the formation of well crystalline oxide layer while NPs are forming a stable passive layer with thickness of about 4 nm [12, 13]. TEM observation of oxide shell thickness shows a good agreement with mentioned theory in [12]. Moreover the formation of the low crystalline oxide shell results in the broadened diffraction peaks of the Fe_3O_4 phase.

The dependence of magnetic properties of NPs on temperature and their mean diameter was investigated (Fig. 3). The saturated magnetization is smaller in compare with bulk counterparts of Fe_3O_4 (MS = 92–100 A m^2/kg) [14]. This can be attributed to the surface disorder or spin canting at the particles surface [15, 16].
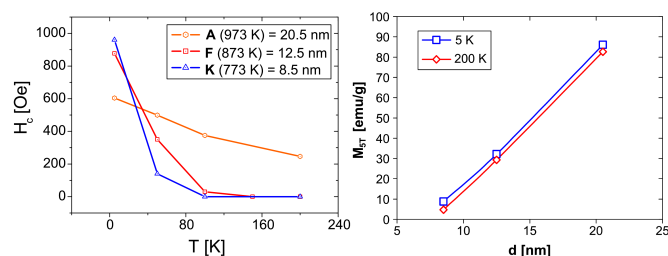
Fig. 3. The temperature dependences of coercivity (left) and the particle size dependences of magnetization $M_{5\ \mathrm{T}}$ measured in magnetic field at 5 T (right).

The coercivity, H_c, was determined from the hysteresis loop measured at temperatures 5, 50, 100, and 200 K. As it can be seen from Fig. 3, the H_c value increases with the decrease of temperature. At lower temperature, it is expected the occurring of blocking effect. The coercivity of 20 nm NPs (sample A) linearly decrease with temperature in measured temperature interval. The coercivity of 12.5 and 8.5 nm NPs (sample F and K) markedly decrease with temperature. At temperature 100 K the dependence change and samples show just slight temperature dependence of H_c. The decrease of H_c (measured at 5 K) with increase of NPs size suggests that above temperatures where $H_c = 0$ A/m (sample F = 150 K and sample K = 200 K) NPs are superparamagnetic. This temperature is referred as blocking temperature.

4. Conclusions

We showed that metallic Fe NPs, with size of 20, 12.5, and 8.5 nm, synthesized by a solid state precipitation method, consist of α-Fe core and Fe_3O_4 shell with thickness of 2–4 nm. The results of average particle size and structure characteristics observed using TEM and SAED are consistent with XRD analysis. The decrease

of the temperature of precipitation annealing causes decrease of the diffusion intensity, so precipitates are smaller and the smallest 8.5 nm NPs consist only of Fe_3O_4. The core-shell NPs have relatively high saturation magnetization (from $M_{5\ \mathrm{T}} = 82.6$ A m^2/kg for 20.5 nm to $M_{5\ \mathrm{T}} = 29.3$ A m^2/kg for 12.5 nm). The crystallite size, α-Fe fraction, and saturation of magnetization decrease with temperature of precipitation annealing. NPs with diameter smaller than ≈ 12.5 nm are superparamagnetic due to thermal fluctuation. These results describe way for production of core-shell particles of various metals that are not currently synthesized in bulk using precipitation from solid state solution.

References

[1] D. Ramimoghadam, S. Bagheri, S.B.A. Hamid, *J. Magn. Magn. Mater.* **368**, 207 (2014).

[2] H. Yan, Ch. You, Z. Song, B. Yu, Y. Shen *Mater. Chem. Phys.* **113**, 46 (2009).

[3] H. Iida, K. Takayanagi, T. Nakanishi, T. Osaka, *J. Coll. Interf. Sci.* **314**, 274 (2007).

[4] C. de Montferrand, L. Hu, I. Milosevic, V. Russier, D. Bonnin, L. Motte, A. Brioude, Y. Lalatonne, *Acta Biomater.* **9**, 6150 (2013).

[5] A. Shavel, L.M. Liz-Marzan, *Phys. Chem. Chem. Phys.* **11**, 3762 (2009).

[6] H. Yang, T. Ogawa, D. Hasegawa, M. Takahashi, *J. Appl. Phys.* **103**, 07D526 (2008).

[7] J. Cheon, N.-J. Kang, S.-M. Lee, J.-H. Lee, J.-H. Yoon, S.J. Oh, *J. Am. Chem. Soc.* **126**, 1950 (2004).

[8] S.-J. Park, S. Kim, S. Lee, Z.G. Khim, K. Char, T. Hyeon, *J. Am. Chem. Soc.* **122**, 8581 (2000).

[9] M. Zhu, G. Diao, *J. Phys. Chem. C* **115**, 18923 (2011).

[10] Q. He, T. Yuan, S. Wei, N. Haldolaarachchige, Z. Luo, D.P. Young, A. Khasanov, Z. Guo, *Angew. Chem. Int. Ed.* **51**, 8842 (2012).

[11] A.P. Hammersley, *FIT2D: An Introduction and Overview*, ESRF Internal Report, ESRF97HA02T, 1997.

[12] K.K. Fung, B. Qin, X.X. Zhang, *Mater. Sci. Eng.* **286**, 135 (2000).

[13] O. Milkovič, G. Janak, S. Niznik, S. Longauer, L. Frohlich, *Mater. Lett.* **64**, 144 (2010).

[14] R. Cornell, U. Schwertmann, *The Iron Oxides*, Wiley-VCH, Weinheim 2003.

[15] C.-R. Lin, Y.-M. Chu, S.-C. Wang, *Mater. Lett.* **60**, 447 (2006).

[16] X. Batlle, A. Labarta, *J. Phys. D Appl. Phys.* **35**, R15 (2002).